

It should be noted that the control law (11.81), (11.82), once mapped back to the original coordinates, is discontinuous at the origin of the configuration space \mathcal{C} . As a matter of fact, it can be proven that any feedback law that can regulate the posture of the unicycle must be necessarily discontinuous with respect to the state and/or time-varying.¹²

Simulations

To illustrate the characteristics of the above regulation schemes, simulation results are now presented for two parking manoeuvres performed in feedback by a unicycle mobile robot.

Figure 11.19 shows the robot trajectories produced by the Cartesian regulator (11.78), (11.79), with $k = 1$ and $k_2 = 3$, for two different initial configurations. Note that the final orientation of the robot varies with the approach direction, and that the unicycle reaches the destination in forward motion, after inverting its motion at most once (like in the second manoeuvre). It is possible to prove that such behaviour is general with this controller.

The results of the application of the posture regulator (11.81), (11.82) starting from the same initial conditions are shown in Fig. 11.20. The gains have been set to $k_1 = 1$, $k_2 = 2.5$ and $k_3 = 3$. The trajectories obtained are quite similar to the previous ones, but as expected the orientation is driven to zero as well. As before, the final approach to the destination is always in forward motion, with at most one motion inversion in the transient phase.

11.7 Odometric Localization

The implementation of any feedback controller requires the availability of the robot configuration at each time instant. Unlike the case of manipulators, in which the joint encoders provide a direct measurement of the configuration, mobile robots are equipped with incremental encoders that measure the rotation of the wheels, but not directly the position and orientation of the vehicle with respect to a fixed world frame. It is therefore necessary to devise a *localization* procedure that estimates in real time the robot configuration.

Consider a unicycle moving under the action of velocity commands v and ω that are constant within each sampling interval. This assumption, which

¹² This result, which actually applies to all nonholonomic robots, derives from the application of a necessary condition (*Brockett theorem*) for the smooth stabilizability of control systems. In the particular case of a driftless system of the form (11.10), in which there are fewer inputs than states and the input vector fields are linearly independent, such a condition is violated and no control law that is continuous in the state \mathbf{q} can asymptotically stabilize an equilibrium point. Brockett theorem does not apply to time-varying stabilizing controllers that may thus be continuous in \mathbf{q} .

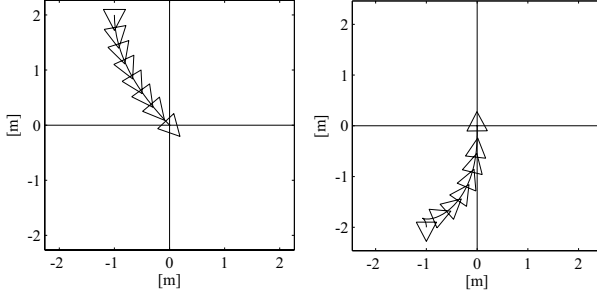


Fig. 11.19. Regulation to the origin of the Cartesian position of the unicycle with the controller (11.78), (11.79), for two different initial configurations

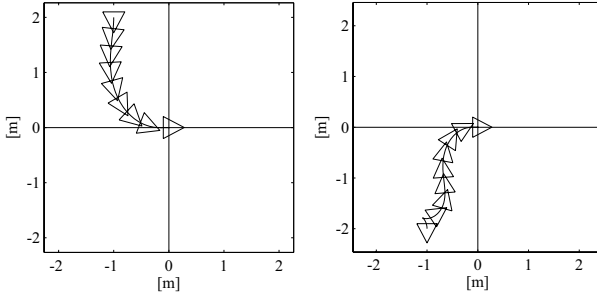


Fig. 11.20. Regulation to the origin of the posture of the unicycle with the controller (11.81), (11.82), for two different initial configurations

is generally satisfied¹³ in digital control implementations, implies that during the interval the robot moves along an arc of circle of radius $R = v_k/\omega_k$, which degenerates to a line segment if $\omega_k = 0$. Assume that the robot configuration $\mathbf{q}(t_k) = \mathbf{q}_k$ at the sampling time t_k is known, together with the value of the velocity inputs v_k and ω_k applied in the interval $[t_k, t_{k+1})$. The value of the configuration variables \mathbf{q}_{k+1} at the sampling time t_{k+1} can then be reconstructed by forward integration of the kinematic model (11.13).

A first possibility is to use the approximate formulae

$$\begin{aligned} x_{k+1} &= x_k + v_k T_s \cos \theta_k \\ y_{k+1} &= y_k + v_k T_s \sin \theta_k \\ \theta_{k+1} &= \theta_k + \omega_k T_s, \end{aligned} \tag{11.83}$$

where $T_s = t_{k+1} - t_k$ is the duration of the sampling interval. These equations, which correspond to the use of the Euler method for numerical integration

¹³ In particular, this is certainly true if the velocity commands computed by the digital controller are converted to control inputs for the robot through a zero-order hold (ZOH).

of (11.13), introduce an error in the computation of x_{k+1} and y_{k+1} , that is performed as if the orientation θ_k remained constant throughout the interval. This error becomes smaller as T_s is decreased. The third formula instead is exact.

If the accuracy of the Euler method proves to be inadequate, one may use the following estimate with the same T_s :

$$\begin{aligned}x_{k+1} &= x_k + v_k T_s \cos \left(\theta_k + \frac{\omega_k T_s}{2} \right) \\y_{k+1} &= y_k + v_k T_s \sin \left(\theta_k + \frac{\omega_k T_s}{2} \right) \\\theta_{k+1} &= \theta_k + \omega_k T_s,\end{aligned}\tag{11.84}$$

corresponding to the adoption of the second-order Runge–Kutta integration method. Note how the first two formulae use the average value of the unicycle orientation in the sampling interval.

To obtain an exact reconstruction of \mathbf{q}_{k+1} under the assumption of constant velocity inputs within the sampling interval one may use simple geometric arguments or exploit the transformability of the unicycle kinematic model in the chained form (11.25). As already seen, this form is easily integrable in closed form, leading to an exact expression for \mathbf{z}_{k+1} . The configuration \mathbf{q}_{k+1} can then be computed by inverting the coordinate and input transformations (11.23) and (11.24). This procedure, which can be generalized to any mobile robot that can be put in chained form, provides the formulae:

$$\begin{aligned}x_{k+1} &= x_k + \frac{v_k}{\omega_k} (\sin \theta_{k+1} - \sin \theta_k) \\y_{k+1} &= y_k - \frac{v_k}{\omega_k} (\cos \theta_{k+1} - \cos \theta_k) \\\theta_{k+1} &= \theta_k + \omega_k T_s.\end{aligned}\tag{11.85}$$

Note that the first two are still defined for $\omega_k = 0$; in this case, they coincide with the corresponding formulae of Euler and Runge–Kutta methods (which are exact over line segments). In the implementation, however, it is necessary to handle this situation with a conditional instruction.

Figure 11.21 allows a comparison among the configurations \mathbf{q}_{k+1} reconstructed via the three aforementioned integration methods. In practice, the difference is obviously much less dramatic, and tends to disappear as the duration T_s of the sampling interval is decreased.

In the previous formulae it has been assumed that the velocity inputs v_k and ω_k applied in the sampling interval are available. In view of the non-ideality of any actuation system, rather than relying on the ‘commanded’ values, it is convenient to reconstruct v_k and ω_k using the robot proprioceptive sensors. First of all, note that

$$v_k T_s = \Delta s \quad \omega_k T_s = \Delta \theta \quad \frac{v_k}{\omega_k} = \frac{\Delta s}{\Delta \theta},\tag{11.86}$$

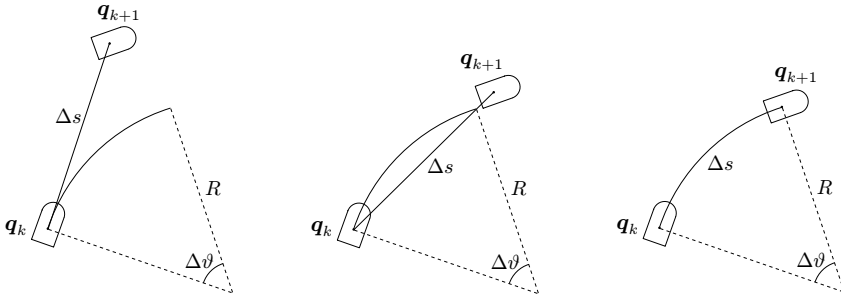


Fig. 11.21. Odometric localization for a unicycle moving along an elementary tract corresponding to an arc of circle; *left*: integration via Euler method, *centre*: integration via Runge–Kutta method, *right*: exact integration

where Δs is the length of the elementary tract travelled by the robot and $\Delta\theta$ is the total variation of orientation along the tract. For example, in the case of a differential drive unicycle, denote by $\Delta\phi_R$ and $\Delta\phi_L$ the rotation of the right and left wheel, respectively, as measured by the incremental encoders during the sampling interval. From (11.14) one easily finds

$$\Delta s = \frac{r}{2} (\Delta\phi_R + \Delta\phi_L) \quad \Delta\theta = \frac{r}{d} (\Delta\phi_R - \Delta\phi_L)$$

that, used in (11.86), allow the implementation of all the previous formulae for the reconstruction of \mathbf{q}_{k+1} .

The forward integration of the kinematic model using the velocity commands reconstructed via the proprioceptive sensors — the encoders of the wheel actuators — is referred to as *odometric localization* or *passive localization* or *dead reckoning* — the latter is a term of uncertain etymology used in marine navigation. This method, relying on the iterated use of the previous formulae starting from an estimate of the initial configuration, provides an estimate whose accuracy cannot be better than that of \mathbf{q}_0 . In any case, odometric localization — independently from the adopted integration method — is subject in practice to an error that grows over time (*drift*) and quickly becomes significant over sufficiently long paths. This error is the result of several causes, that include wheel slippage, inaccuracy in the calibration of kinematic parameters (e.g., the radius of the wheels), as well as the numerical error introduced by the integration method, if Euler or Runge–Kutta methods are used. It should also be noted that, once an odometric localization technique has been chosen, its performance also depends on the specific kinematic arrangement of the robot; for example, differential drive is usually better than synchro drive in this respect.

A more robust solution is represented by *active localization* methods. For example, this kind of approach can be adopted when the robot is equipped with proximity exteroceptive sensors (like a laser range finder) and knows a

map of the workspace, either given in advance or built by the robot itself during the motion. It is then possible to correct the estimate provided by the passive localization methods by comparing the expected measures of the exteroceptive sensors with the actual readings. These techniques, which make use of tools from *Bayesian estimation theory* such as the *Extended Kalman Filter* or the *Particle Filter*, provide greater accuracy than pure odometric localization and are therefore essential in navigation tasks over long paths.

Bibliography

The literature on mobile robots is very rich and includes some comprehensive treatises, among which one of the most recent is [210].

Many books deal with the realization of mobile robots, with particular emphasis on electro-mechanical design and sensor equipment, e.g., [106, 72, 21]. For the modelling of systems subject to nonholonomic constraints, see [164]. A general classification of wheeled mobile robots based on the number, placement and type of wheels is proposed in [18], where the derivation of the kinematic and dynamic models is also presented.

Conditions for transforming driftless systems in chained form are discussed in detail in [159], while a general reference on flat outputs is [80]. The presented schemes for Cartesian trajectory tracking based on linear and nonlinear control are taken from [34], while the method for posture regulation based on polar coordinates was proposed in [2]. Complete (input/state) linearization of the unicycle kinematic model can be obtained using a dynamic feedback law, as shown for example in [174]. The non-existence of a universal controller for nonholonomic robots is proven in [135].

A detailed extension of some of the planning and control techniques described in this chapter to the case of bicycle-like kinematics is given in [58]. The design of time-varying and/or discontinuous feedback control laws for posture regulation in mobile robots was addressed in many works, including [193] and [153].

The reader interested in sensor-based robot localization and map building can refer, e.g., to [231].

Problems

11.1. Consider the mobile robot obtained by connecting N trailers to a rear-wheel drive tricycle. Each trailer is a rigid body with an axle carrying two fixed wheels, that can be assimilated to a single wheel located at the midpoint of the axle, and is hinged to the midpoint of the preceding axle through a revolute joint. Find a set of generalized coordinates for the robot.